Inorganica Chimica Acta 509 (2020) 119681

Contents lists available at ScienceDirect

Inorganica Chimica Acta

journal homepage: www.elsevier.com/locate/ica

Research paper

Visible light generation of chromium(V)-oxo salen complexes and mechanistic insights into catalytic sulfide oxidation

Seth Klaine, Ngo Fung Lee, Angeline Dames, Rui Zhang*

Department of Chemistry, Western Kentucky University, Bowling Green, KY 42101-1079, USA

ARTICLE INFO

Keywords:
Chromium(V)-oxo
Salen
Visible light
Oxidation
Kinetics

ABSTRACT

Visible light irradiation of the photo-labile salen-chromium(III) chlorate or bromate precursors produced salen-chromium(V)-oxo complexes that were spectroscopically and kinetically indistinguishable from those formed by chemical oxidation of chromium(III) salens with $PhI(OAc)_2$. The photochemistry observed in this work is ascribed to the *heterolytic* cleavage of the O-X bond in the apical counterion that results in a two-electron oxidation of the metal to form the chromium(V)-oxo species. Second-order rate constants for oxidation reactions of **3** with organic substrates were determined under pseudo-first order condition, and particularly low level of reactivity for sulfide oxidations was observed. In this study, chromium(III) salen complexes effectively catalyzed the oxidation of aryl sulfides into sulfoxides with $PhI(OAc)_2$ in the presence of a small amount of water. The competition product studies with the Hammett correlation plot indicated that the observed chromium(V)-oxo species is not likely to serve as the major oxidant for the sulfide oxidations catalyzed by chromium(III) salens with $PhI(OAc)_2$.

1. Introduction

In industry and laboratories, the catalytic oxidation of organic compounds is one of most important processes conducted daily on a large scale for the production of valuable chemicals, remediation of pollutants, and the production of energy [1–4]. Meanwhile, oxidations mediated by a variety of enzymes play a key role in the oxidative transformation of endogenous and exogenous molecules in all forms of life [5]. An ubiquitous type of monooxygenase is cytochrome *P*-450 enzymes (P450s) that contain a metalloporphyrin core and catalyze a wide variety of oxidation reactions with exceptionally high reactivity and selectivity [6,7]. Many synthetic metal complexes have been synthesized to develop enzyme-like oxidation catalysts [8–13]. In this context, metallosalen complexes (salen = *N,N'*-bis(salicylidene)ethylenediamine) have received considerable attention in view of their enormous utility of catalytic transformations [14–17]. With tetradentate-binding motif, metallosalens have features in common with metalloporphyrins with respect to their catalytic properties [18]. Notably, metal-salen complexes are more easily synthesized and manipulated to create an asymmetric environment around the active metal site than porphyrin analogues [18,19]. In the 1990s, the groups of Jacobsen and Katsuki independently introduced chiral manganese–salen catalysts to achieve highly enantioselective epoxidations [20,21]. To date, the Jacobsen–Katsuki catalysts are accepted as one of the most successful and widely applicable methods for the epoxidation of unfunctionalized olefins [22,23].

Despite great success in catalytic transformations, mechanistic elucidation of these salen systems have so far been hampered by the fact that the catalytically active species appear only as fleeting putative intermediates [18,24]. The mechanistic scheme adopted for oxygen atom transfer to organic substrates by salen complexes is mainly based on the isolation and characterization of a chromium(V)-oxo species [14]. Limited evidence for the existence of most salen-metal-oxo species is responsible for the lack of mechanistic insights [25,26]. In this regard, we recently introduced visible light-induced ligand cleavage reactions that successfully generated a variety of metal-oxo species supported by porphyrin and corrole ligands [27–32]. Unlike the commonly used chemical oxidations, the use of visible light (sunlight) rather than a chemical reagent offers an ideal means to produce metal-oxo species with much higher temporal resolution, and permits direct studies of their oxidation reactions in real time [33–35]. In addition, kinetics of oxidation reactions of the photo-generated transients of interest are not convoluted with the kinetics of reactions that form the transients from chemical methods [36]. With the aim to probe the nature of active oxidizing species and elucidate mechanistic courses in metal-salen catalysis, we have applied the promising photo-induced ligand cleavage approaches to generate salen-metal-oxo intermediates. Herein, we report our ongoing progress on visible light-generation of chromium(V)-

---

* Corresponding author.
E-mail address: rui.zhang@wku.edu (R. Zhang).

https://doi.org/10.1016/j.ica.2020.119681
Received 28 February 2020; Received in revised form 9 April 2020; Accepted 15 April 2020

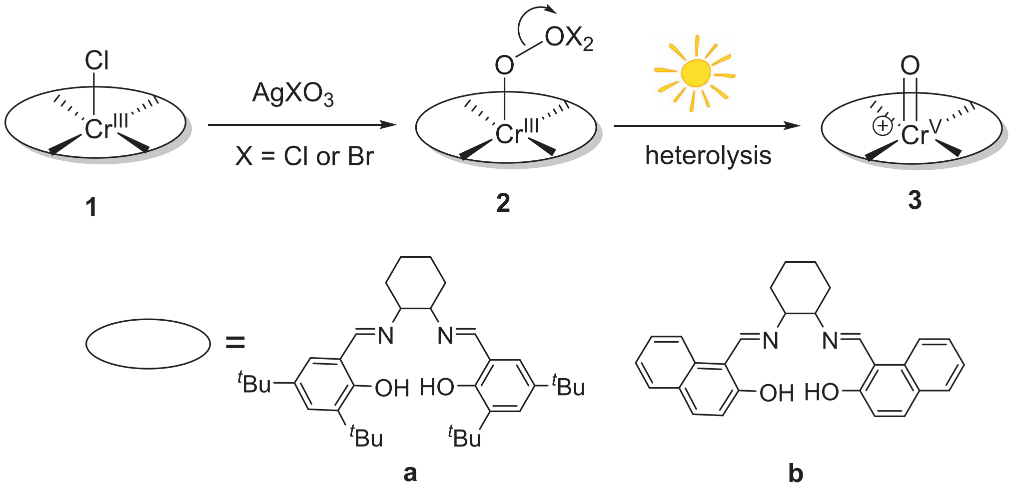

Scheme 1. Visible light-induced formation of salen-chromium(V)-oxo complexes.

oxo complexes bearing the well-known Jacobsen salen ligand and one of its derivatives (Scheme 1). The results attest to the fact, for the first time, that photochemical production of metal-oxo species is not exclusive to porphyrin or corrole systems, and it can be achieved using simple, easily constructed salen-based complexes. Meanwhile, we report rate constants for the reactions of generated salen-chromium(V)-oxo intermediates with organic substrates. The kinetic and competition studies provide mechanistic insights into the identity and reactivity of the active oxidant involved in the catalytic sulfide oxidations.

2. Experimental

2.1. Materials and instruments

All commercial reagents were of the best available purity and were used as supplied unless otherwise specified. Acetonitrile was obtained from Sigma Aldrich (HPLC grade) and use as such. All organic substrates for kinetic studies were passed through a flash chromatography column of active alumina (Grade I) before use. Cr^{III}(salen)Cl (**1a**) (salen = *N,N′*-bis(3,5-di-*tert*-butylsalicylidene)-1,2-cyclohexanediamino) was purchased from Sigma Aldrich and use without further purification. Complex **1b** (salen = *N,N′*-bis-(2-hydroxy-1-naphthalidene)-1,2-cyclohexanediamine) was prepared according to the well-established procedure [37] and its purity was checked by UV–vis and ^{1}H NMR.

UV–Vis spectra were conducted on an Agilent 8454 diode array spectrometer using standard 1.0-cm quartz cuvettes. Visible light was produced from a SOLA SE II light engine (Lumencor) configured with a liquid light guide (output power ranging from 6 to 120 W). Electrospray ionization-mass spectroscopy (ESI-MS) data was collected using an Agilent 500 LCMS Ion Trap System. Kinetic measurements were performed on an Agilent 8454 diode array spectrophotometer using standard 1.0-cm quartz cuvettes.

2.2. General procedure for synthesis of chromium(V)-oxo salens

Axial ligand exchange of the salen complexes [Cr^{III}(salen)Cl] (**1**) with excess of Ag(ClO$_3$) or Ag(BrO$_3$) in CH$_3$CN or CH$_2$Cl$_2$ gave the corresponding chlorate or bromate complexes [Cr^{III}(salen)(XO$_3$)] (X = Cl or Br) (**2**), which were photo-labile and subsequently used for photochemical reactions. The solution of **2** with concentration of ca. 1.0×10^{-3} M was irradiated with visible light from a SOLA engine (output power 120 W) at ambient temperature. The formation of chromium(V)-oxo salen complexes (**3**) was complete in the range of 12 to 15 min, as monitored by UV–vis spectroscopy. The photo transformation is characterized by a distinct color changes from yellow to dark green, and accompanied by the formation of a broad peak from 550 to 800 nm. Following previous work, the same [Cr^{V}(salen)(O)] was also produced by chemical oxidation of precursors **1** with PhI(OAc)$_2$ (2.5–5 equiv.) as the sacrificial oxidant, and the time-resolved absorption spectra exhibited the same characteristic broad peak.

2.3. Kinetic studies of chromium(V)-oxo salens

Reactions of high-valent salen-chromium(V)-oxo species with excess amounts of organic substrates were conducted in solutions at 23 ± 2 °C. The approximate concentrations of **3** were estimated by assuming 100% conversion of chromium(III) precursor in the photochemical reactions. The rates of the reactions which represent the rates of oxo group transfer from [Cr^{V}(salen)(O)] to substrate were monitored by the decay of the broad absorption band of the oxo-species **3**. The kinetic traces at λ_{max} of 680 nm displayed good pseudo-first-order behavior for at least four half-lives, and the data was solved to give pseudo-first-order observed rate constants, k_{obs}. Plots of these values against the concentration of substrate were linear in all cases. The second-order rate constants for reactions of the oxo species with the organic substrates were solved according to Eq. (1), where k_0 is a background rate constant found in the absence of added substrate, k_{ox} is the second-order rate constant for reaction with the substrate, and [Sub] is the concentration of substrate. Most second-order rate constants are averages of 2–3 determinations consisting of 3 independent kinetic measurements. Errors in the rate constants were weighted and are at 2σ.

$$k_{obs} = k_0 + k_{ox}[\mathrm{Sub}] \qquad (1)$$

2.4. General procedure for catalytic sulfoxidations

Unless otherwise indicated, all catalytic reactions were typically carried out in a 10 mL reaction vial which was charged with the catalyst (10 μmol, 2.0 mol%), sulfide substrate (0.5 mmol) in methanol (2 mL) with a small amount of H$_2$O (5.0 μL). PhI(OAc)$_2$ (0.75 mmol) was then added at 23 °C to trigger the reactions. Aliquots of the reaction solution at constant time interval were diluted (> 200 times) and analyzed by GC/MS to determine the formed products with an internal standard (1,2,4-trichlorobenzene). The conversions were calculated based on the substrate consumed and the selectivities based on the percentage ratios of sulfoxides and sulfones, which were only oxidized products detected. All reactions were run 2 to 3 times, and the data reported represent the average of these reactions. Products including sulfoxides and sulfones from the over oxidation were identified by GC–MS. Since the sulfoxidation reactions were not affected by molecular oxygen, all the reactions presented in Table 2 were performed in air under ambient light.

2.5. Competition and Hammett correlation studies

A CH_3OH solution containing equal amounts of two substrates, e.g. thioanisole (0.2 mmol) and substituted thioanisoles (0.2 mmol), chromium(III) salen catalyst (10 μmol) and an internal standard of 1,2,4-trichlorobenzene (0.1 mmol) was prepared (final volume = 2.0 mL). $PhI(OAc)_2$ (0.1 mmol) as the limiting reagent, was added and the mixture was stirred at ambient temperature (23 ± 2 °C) in the presence of a small amount of H_2O (5.0 μL) for 10 to 20 min. Relative rate ratios for catalytic oxidations were determined by GC based on the amounts of sulfoxide products as measured against an internal standard. In this work, all the catalytic sulfoxidations proceeded with good yields (> 95%). Thus, the ratio of product formation should reasonably reflect the relative sulfide reactivity toward the salen-chromium(III)-catalyzed oxidations.

3. Results and discussion

3.1. Visible light photolysis of $[Cr^{III}(salen)(ClO_3)]$ and $[Cr^{III}(salen)(BrO_3]$

As shown in Scheme 1, treatment of $Cr^{III}(salen)Cl$ (**1a**) with excess $Ag(ClO_3)$ (10 equiv.) resulted in rapid exchange of the axial ligand to form the corresponding chlorate $Cr^{III}(salen)(ClO_3)$ (**2a**) with observation of AgCl precipitate. The formation of **2a** was further indicated by the UV–vis spectra with a blue-shifted Soret band at 422 nm (Fig. 1A). Species **2a** was highly photo-labile and thus, not isolated and immediately used for photochemical reactions after preparation. Irradiation of chlorate complex **2a** in anaerobic CH_3CN with visible light from a SOLA engine (output power 60 W) resulted in formation of a new species with a distinct color change. Over a period of 12 min., the yellow species **2a** was decayed and a *dark-green* species **3a** was formed (Fig. 1A), exhibiting a broad band ranging from 550 to 800 nm that is characteristic for chromium(V)-oxo salen complexes [14]. The photo-generated **3a** was metastable and can be further characterized by ESI-MS. As shown in the inset of Fig. 1A, the ESI-MS spectrum (positive mode) exhibited a prominent peak at a mass-to-charge ratio (*m/z*) of 612, matching the molecular composition of $[Cr(salen)(O)]^+$. Accordingly, species **3a** was assigned as $[Cr^V(salen)(O)](ClO_3)$ on the basis of its distinct UV–vis absorption and ESI-MS. The spectra signature of the chromium(V)-oxo salen was further confirmed by production of the same species in the mixing chemical oxidation of **1a** with a mild oxidant of $PhI(OAc)_2$ (Fig. 1B). It is noteworthy that the presence of donor ligands such as excess pyridine *N*-oxide (pyNO) in this study led to the formation of $[Cr^V(salen)(O)](pyNO)$ with the well-defined broad band extending beyond 800 nm in the visible absorption spectrum [14].

Control experiment showed that species **3a** was not formed in the absence of light. As expected, the transformation of **2a** to **3a** was more rapid using more intensive visible light (120 W). The use of the non-coordinating solvents such as $CHCl_3$ gave similar results (data not shown). However, no formation of **3a** was observed in CH_3OH solution. Clearly, the relatively chlorate bound to chromium metal can be readily disassociated by the strong coordinating solvent. As monitored by UV–vis spectroscopy, we did not observe any significant photo-degradation of the complexes in all studies under visible light irradiation. Of note, the long tail band of photo-generated **3a** was not significantly changed when adding pyridine *N*-oxide as the additional donor ligand.

Visible light irradiation of salen-chromium(III) bromate also gave the formation of species **3a** in a faster rate (see Fig. 2A), implying a more efficient photochemical process. In a fashion similar to that described for the generation of **3a**, **3b** with a derived salen ligand (*N,N′*-bis-(2-hydroxy-1-naphthalidene)-1,2-cyclohexanediamine) was also formed by visible light photolysis of corresponding chlorate or bromate precursors (Fig. 2B). Again, the spectral signature of product **3b** was further confirmed by forming same species with the characteristic broad bands from 600 to 800 nm from the chemical oxidation of **1b** by $PhI(OAc)_2$.

Photolysis of porphyrin-$Mn^{III}(ClO_4)$ complexes was previously reported to give porphyrin-$Mn^V(O)$ species by heterolytic cleavage of an O-Cl bond [33]. Recent studies showed that heme iron(III)–hydroperoxo complexes thermodynamically led through a heterolytic O—O bond cleavage to a high-valent iron(IV)–oxo heme cation radical intermediate [38]. Our photolysis studies of porphyrin–iron(III) bromates also showed that the electron-releasing porphyrin system favored a heterolysis of O-Br bond to give porphyrin-iron(IV)-oxo radical cations (compound I models) [29,39]. Thus, the generation of the chromium(V)-oxo species **3** upon visible light irradiation of chlorate or bromate **2** can be rationalized by photo-induced *hetereolytic* cleavage of O-X (X = Cl or Br) bonds in the apical counterion, which results in two-electron photo-oxidation reactions as expected. For comparison, we found that photochemical cleavage of the bromate complexes was considerably more efficient than cleavages of chlorate complex to generate the salen-chromium(V)-oxo species under identical conditions, similar to our previously reported work on the photochemical formation of *trans*-dioxoruthenium(VI) porphyrins [40].

3.2. Kinetic studies of $[Cr^V(salen)(O)]$ species

As expected, photo- and chemical-generated salen-chromium(V)-oxo species **3** is reactive towards organic substrates, and its characteristic broad peak with λ_{max} at 680 nm undergoes exponential decay at a

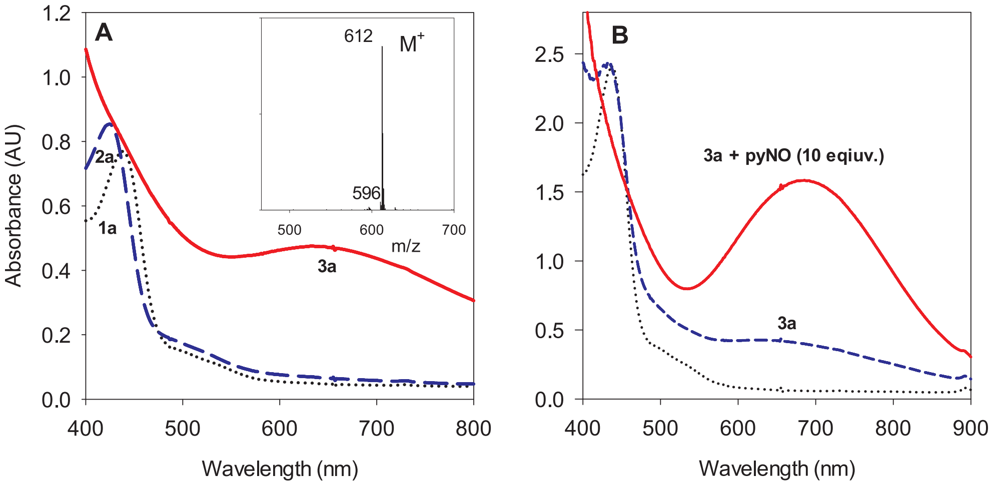

Fig. 1. (A) UV–visible spectrum: $[Cr^{III}(salen)Cl]$ (**1a**, dotted) and $[Cr^{III}(salen)(ClO_3)]$ (**2a**, dash), and $[Cr^V(salen)(O)](ClO_3)$ (**3a**, solid) formed upon visible light photolysis of **2a** in CH_3CN; Inset showing ESI-MS spectrum of photo-generated **3a** in a positive mode. (B) UV–visible spectrum: **1a** (dashed), **3a** formed by oxidation of **1a** with $PhI(OAc)_2$ (2.5 equiv.) in CH_3CN, and the adduct of **3a** (solid) in the presence of pyridine *N*-oxide (10 equiv.)

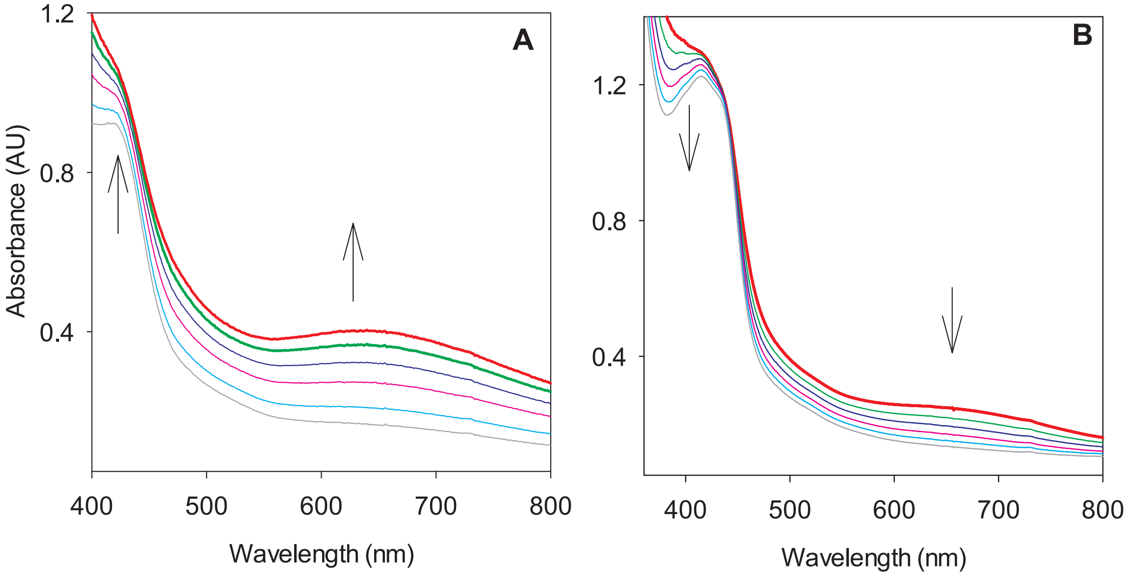

Fig. 2. (A) Time-resolved formation spectra of **3a** (red line) following irradiation of [Cr^{III}(salen)(BrO_3)] (1.0 mM) over 5 min with visible light in anaerobic CH_3CN at 23 °C; (B) Time-resolved spectra of the photo-generated **3b** decaying in the absence of substrate in CH_3CN over 10 min. (For interpretation of the references to color in this figure legend, the reader is referred to the web version of this article.)

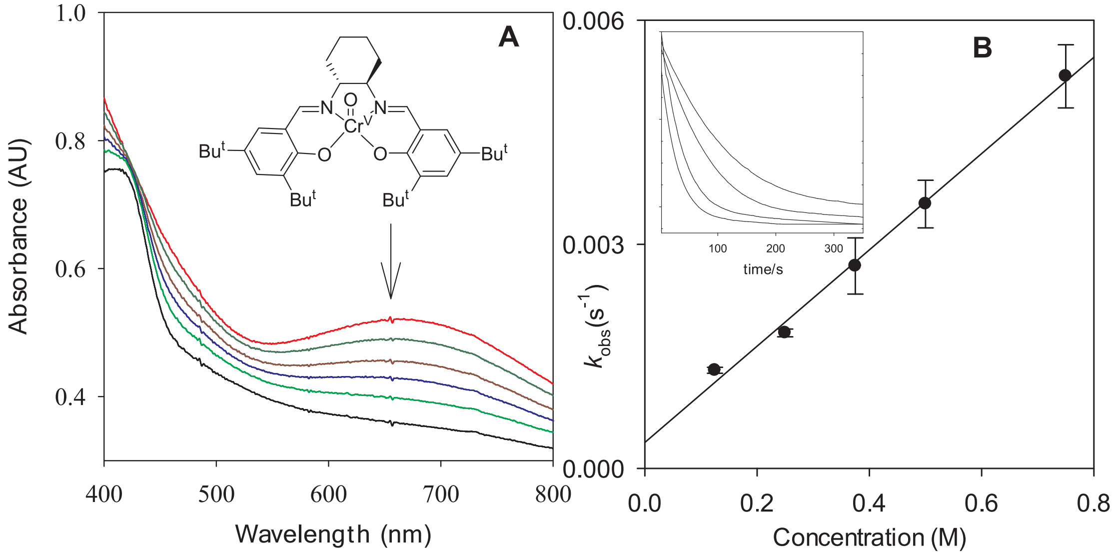

Fig. 3. (**A**) Time-resolved spectra of the photo-generated **3a** reacting with cyclohexene (0.15 M) in CH_3CN over 10 min. (**B**) Kinetic plot of observed rate constants versus concentration of cyclohexene. Inset shows the kinetic traces at 680 nm for the reactions of **3a** with cyclohexene at different concentrations (0.15, 0.25, 0. 5 and 0.75 M from the top to bottom).

Table 1

Second-order rate constants for chromium(V)-oxo salens **3**[a].

Entry	Substrate	k_{ox} ($M^{-1}s^{-1}$) × 10^3	
		3a	**3b**
1	cyclohexene	8.7 ± 0.9	35.0 ± 1.5
	diphenylmethane	33.0 ± 3.0	70.0 ± 6.0
2	1-phenylethanol	32.0 ± 3.0	78.5 ± 10.0
3	thioanisole	0.41 ± 0.02	58.5 ± 6.0
4	4-fluorothioanisole	1.1 ± 0.08	
5	4-chlorothioanisole	0.33 ± 0.02	
6	4-methylthioanisole	0.37 ± 0.04	
7	4-methoxylthioanisole	0.37 ± 0.02	

[a] Generated either by photochemical or chemical methods in CH_3CN at 23 ± 2 °C. Reported values are the average of 2–3 runs with a deviation of 2σ.

rate dependent on the nature and concentration of the organic substrate, permitting direct kinetic studies of their oxidations. In the presence of organic substrate such as cyclohexene, the time-resolved spectra show the clean conversion of **3a** to regenerate the chromium (III) species (**1a**) with a λ_{max} of 420 nm (see Fig. 3A). In kinetic studies, we monitored the absorbance in the Q band region at 680 nm that decayed over the course of reaction (Inset in Fig. 3B). The traces were fit to single-exponential decay, as expected for reactions under pseudo-first-order conditions. When organic substrates such as cyclohexene were present, the decay of photochemically generated species **3a** accelerated linearly with the substrate concentrations with a near-zero intercept (Fig. 3B). The plot slope gave a second-order rate constant of (8.7 ± 0.9) × $10^{-3}\,M^{-1}\,s^{-1}$, almost identical to the k_{ox} for oxidant **3a** produced from chemical oxidation by PhI(OAc)$_2$. Rate constants for the reactions of other organic substrates with generated oxo species **3** were collected in the Table 1.

Table 2
Catalytic oxidation of thioanisoles by chromium(III) salens (1) and $PhI(OAc)_2$.[a]

Entry	Catalyst	Substrate	Time (min)	Conv.[b] (%)	Product	Selectivity%[b] (sulfoxide : sulfone)
1	**1a**	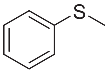	30	100	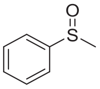	91:09
2	**1b**	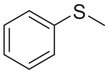	10	100	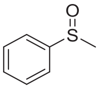	85:15
3[c]	**1a**	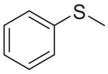	30	100	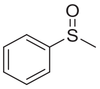	92:08
4	**1a**	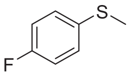	60	99	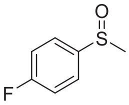	87:13
5	**1a**	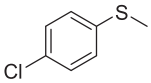	60	100	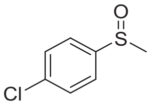	89:11
6	**1a**	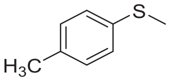	20	92	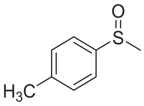	84:16
7	**1a**	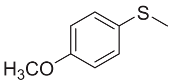	20	97	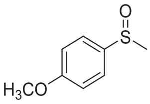	92:08

[a] Unless otherwise specified, all reactions were performed in CH_3OH (2 mL) at ca. 23 °C with 1.5 equiv. of $PhI(OAc)_2$ (0.75 mmol), sulfide substrate (0.5 mmol), 2.0 mol% catalyst in the presence of H_2O (5.0 μL). In all cases, only sulfoxides and small amounts of sulfone were detected by GC–MS analysis of the crude reaction mixture.

[b] Based on the substrate consumed and products ratios determined by GC–MS analysis on the crude reaction mixture after the reaction; material balance > 95%. [c] Carried out in the presence of pyridine *N*-oxide.

Inspection of Table 1 revealed several noteworthy aspects of the salen-chromium(V)-oxo kinetics. It is clear to note the difference in the reactivity of two different $[Cr^V(salen)(O)]$ complexes toward the same substrate, i.e. the less sterically encumbered complex **3b** reacted faster with a given substrate than the complex **3a**, apparently due to steric effects. Although both complexes have essentially the similar square-pyramidal configuration about the chromium(V) center, **3b** carries a more conjugated and planar naphthalene structure than **3a**. Of note, thioanisoles exhibited lower level of reactivity in comparison to hydrocarbons such cyclohexene and diphenylmethane (Ph_2CH_2). In general, a remarkable rate acceleration of sulfide oxidation versus hydrocarbons by electrophilic metal-oxo species is expected in view of the enhanced nucleophilicity and easy access of sulfur for oxidation. For example, our previously studies with iron(IV)-oxo porphyrins [41] and manganese(V)-oxo corroles [30] showed that sulfoxidation reactions were 3 to 4 orders of magnitude faster than those alkene and activated C—H bonds oxidations by the same oxo species. However, the k_2 values determined in this work did not show such rate acceleration of sulfide oxidation by salen-chromium(V)-oxo species, reflecting the operation of a different mechanism for sulfide oxidations. The small rate constants observed in this study suggested the sulfide oxidation did not proceed through nucleophilic attack of sulfide on the chromium center, as it is difficult to generate the sulfoxide through that formation [42]. Indeed, the strong coordination of the sulfides to the metal center suppressed the reactivity of electrophilic salen-chromium(V)-oxo species.

For a given oxo species (**3a**), we observed a small kinetic effect that the substituent at *para*-phenyl position of substrates has on the rates of reactions at room temperature, and the second-order rate constants for the oxidation of *para* substituted thioanisoles typically showed little variation (Table 1, entries 4–7), except that only 4-fluorothioanisole showed increased reactivity in comparison to other substituted thioanisoles. The kinetic data from the reaction of *para*-substituted thioanisoles with **3a** permitted Hammett analysis. However, there is no linear correlation between the $\log k_{rel}$ [$k_{rel} = k(\text{substituted thioanisole})/k(\text{thioanisole})$] and σ or σ^+, implying that no appreciable charge developed on the sulfur during the oxidation process by chromium(V)-oxo species. Of note, non-linear Hammett plots have also been observed for the reactions of *para*-substituted thioanisoles with *trans*-dioxoruthenium(IV) and iron(IV)-oxo porphyrins [41,43], which were ascribed to substantial development of radical character in the transition states.

3.3. Catalytic and competition studies of sulfoxidation reactions

The selective oxidation of organic sulfide to sulfoxide (sulfoxidation) is of importance particularly in the preparation of optically active sulfoxides for a variety of medicinal and pharmaceutical compounds [44]. To date, various catalysts including polyoxometalates have been reported in the literature for the catalytic oxidation of sulfides commonly with H_2O_2 [45–47]. Recently we and others have found that $PhI(OAc)_2$ with a small amount of water is an efficient oxygen source for metalloporphyrins and metallocorroles catalyzed oxidations [48–52]. According to these studies, the trace amount of water can induce the steady and slow formation of more oxidizing PhIO from the $PhI(OAc)_2$, at the same time, allow for the release of the stable AcOH (detected by GC) instead of anhydride Ac_2O under anhydrous conditions, thus, resulting in an accelerated reaction.

In this study, we also found that chromium(III) salens catalyzed highly efficient oxidation of aryl sulfides. Under previously established conditions in methanol solutions [53], thioanisoles can be efficiently oxidized with quantitative conversions and the good chemoselectivity for sulfoxides versus sulfones (Table 2, entry1). In comparison, **1b**

Table 3
Relative rate constants from kinetic studies and competition catalytic oxidations.[a]

Substrates	Method	k_{rel}[b]
p-F-PhSMe/PhSMe	kinetic results	2.68
	$PhI(OAc)_2$	0.40
p-Cl-PhSMe/PhSMe	kinetic results	0.80
	$PhI(OAc)_2$	0.23
p-Me-PhSMe/PhSMe	kinetic results	0.90
	$PhI(OAc)_2$	2.36
p-MeO-PhSMe/PhSMe	kinetic results	0.90
	$PhI(OAc)_2$	6.30

[a] A reaction solution containing equal amounts of two substrates, e.g., thioanisole (0.2 mmol) and substituted thioanisole (0.2 mmol), manganese(III) porphyrin catalyst (10 μmol) and an internal standard of 1,2,4-trichlorobenzene was prepared in CH_3OH (2 mL). Iodobenzene diacetate $PhI(OAc)_2$ (0.1 mmol) was added with 5.0 μL H_2O, and the mixture was stirred for *ca*. 10 to 15 min at 23 ± 2 °C.

[b] Relative ratios of absolute rate constants from kinetic results with chromium(V)-oxo salen complex (**3a**) and for competitive oxidations with the chromium(III) salen catalyst (**1a**) at ambient temperature.

showed higher catalytic activity albeit with reduced selectivity for sulfoxide under identical conditions (entry 2). Addition of pyridine *N*-oxide (10 equiv. to the catalyst) showed no appreciable effect on the reactivity and selectivity of the products (entry 3). Control experiments showed that no oxidized products (< 1% by GC) was formed in the presence of $PhI(OAc)_2$ and water without catalyst. Of note, use of other solvents such as CH_3CN, $CHCl_3$ and CH_2Cl_2 resulted in a reduced reactivity in comparison to MeOH (data not shown here). Under the usual catalytic conditions, monitoring reaction by UV–vis spectroscopy before and after reactions indicated that no significant degradation of the salen catalysts was found after catalytic reactions. Similar to our previous studies [49,51], the excellent catalytic activities for sulfide oxidations is rationalized in part by the enhanced stability of chromium salens against the catalytic degradation by using the mild oxygen source. In a sharp contrast, a sluggish reactivity (< 10% convn) was observed after 12 h for the unfunctionalized alkene such as cyclohexene or styrene (data not shown).

In the catalytic oxidation of substituted thioanisoles, we observed a significant effect of substituents in the aryl ring of substrates. As evident in the courses of substituted thioanisole oxidations, the introduction of electron-donating groups like methyl or methoxy groups resulted in increased reactivities compared to thioanisole, while reduced reactivities were observed in the presence of electron-demanding groups like Cl or F groups (entries 4–7 in Table 2). To assess the nature of the active oxidant involved in the catalytic reactions, the competitive studies of sulfoxidations catalyzed by the chromium(III) salen (**1a**) with $PhI(OAc)_2$ as sacrificial oxygen source were conducted as described in experimental section. Notably, the log k_{rel} [$k_{rel} = k$(substituted thioanisole)/k(thioanisole)] versus Hammett substituent constant (σ_p) gave an excellent linear correlation ($R = 0.99$) for the catalytic oxidation of substituted sulfides under competitive conditions. The slope (ρ) of the plot is −2.73, which indicates transition states for rate-limiting steps of sulfide oxidation involves a significant development of positive charge.

As described early in Fig. 1B, $PhI(OAc)_2$ was able to oxidize the chromium(III) complexes (**1**) to produce salen-chromium(V)-oxo **3**, which then reacted with substrate and decayed back to chromium(III) product. Catalytic aerobic oxidation that relies on a corrole-based chromium(V)-oxo/chromium(III) cycle was also known [54]. However, the directly observed salen-chromium(V)-oxo species **3** in above kinetic studies is not necessarily the active oxidant under catalytic turnover conditions. As evident in Table 3, the ratios of absolute rate constants found in direct kinetic studies differed dramatically from the oxidation ratios for competition oxidation reactions of the two substrates under turnover conditions. The obvious explanation for this behavior is that the directly observed chromium(V)-oxo species **3** is not the active oxidant under catalytic turnover conditions [55]. Reaction of the salen-chromium(III) catalysts with the sacrificial oxidant $PhI(OAc)_2$ possibly formed a more reactive intermediate to oxidize the sulfide substrate through a different mechanism. Alternatively, the chromium(V)-oxo salen may function as Lewis acid to activate the $PhI(OAc)_2$ in a similar way as the stable corralizine-manganese(V)-oxo served in the catalytic sulfoxidation with PhIO [56]. A clear mechanism of catalytic sulfoxidation by chromium salen with $PhI(OAc)_2$ requires the definitive detection and characterization of the elusive oxidant that is the direction for future studies.

4. Conclusion

In conclusion, we report here a new and facile photochemical entry to produce and study high-valent salen-chromium(V)-oxo derivatives by visible light irradiation of the corresponding chromium(III) chlorate or bromate complexes. The photochemistry observed in this work is rationalized by the heterolytic cleavage of the O-X bond in the apical counterion that results in a two-electron oxidation to afford the chromium(V)-oxo species. We have confirmed the photo-generated [Cr^V(salen)(O)] is spectroscopically and kinetically indistinguishable from the species formed by the chemical oxidation of chromium(III) precursors with $PhI(OAc)_2$. The small second-order rate constants for sulfide oxidations along with competition product studies in this work suggested that the observed chromium(V)-oxo species in kinetic studies is unlikely to serve as the major oxidant for the catalytic sulfide oxidations by chromium(III) salen catalysts with $PhI(OAc)_2$. On the basis of these findings, we anticipate that analogous salen-metal-oxo species such as manganese(V)-oxo salens could be photochemically generated and kinetically studied in more important alkene expoxidation and C—H bond oxidation, which is currently under investigation in our laboratory.

Conflicts of interest

There are no conflicts to declare.

CRediT authorship contribution statement

Seth Klaine: Investigation, Methodology, Validation. **Ngo Fung Lee:** Methodology, Investigation. **Angeline Dames:** Investigation. **Rui Zhang:** Conceptualization, Project administration, Supervision, Funding acquisition, Writing - review & editing.

Acknowledgments

We greatly acknowledge the National Science Foundation (CHE 1764315) for support of this research. S. Klaine is thankful to the WKU Office of Research and Graduate Studies for awarding internal grants (FUSE and GSRG).

References

[1] A.E. Shilov, G.B. Shulpin, Activation of C-H bonds by metal complexes, Chem. Rev. 97 (1997) 2879–2932.
[2] J.E. Baeckvall, Modern oxidation methods, Wiley-VCH Verlag, Weinheim, 2004.
[3] R.A. Sheldon, Recent advances in green catalytic oxidations of alcohols in aqueous media, Catal. Today 247 (2015) 4–13.
[4] C. He, J. Cheng, X. Zhang, M. Douthwaite, S. Pattisson, Z. Hao, Recent advances in the catalytic oxidation of volatile organic compounds: a review based on pollutant sorts and sources, Chem. Rev. 119 (2019) 4471–4568.
[5] M. Sono, M.P. Roach, E.D. Coulter, J.H. Dawson, Heme-containing oxygenases, Chem. Rev. 96 (1996) 2841–2887.
[6] P.R. Ortiz de Montellano, Cytochrome P450 Structure, Mechanism, and Biochemistry, Kluwer Academic/Plenum, New York, 2005.
[7] I.G. Denisov, T.M. Makris, S.G. Sligar, I. Schlichting, Structure and chemistry of cytochrome P 450, Chem. Rev. 105 (2005) 2253–2277.
[8] B. Meunier, Metalloporphyrins as versatile catalysts for oxidation reactions and

oxidative DNA cleavage, Chem. Rev. 92 (1992) 1411–1456.

[9] T. Punniyamurthy, S. Velusamy, J. Iqbal, Recent advances in transition metal catalyzed oxidation of organic substrates with molecular oxygen, Chem. Rev. 105 (2005) 2329–2363.

[10] C.-M. Che, J.-S. Huang, Metalloporphyrin-based oxidation systems: from bioimetic reactions to application in organic synthesis, Chem. Commun. 3996–4015 (2009).

[11] A.B. Sorokin, Phthalocyanine metal complexes in catalysis, Chem. Rev. 113 (2013) 8152–8191.

[12] S. Sahu, D.P. Goldberg, Activation of dioxygen by iron and manganese complexes: a heme and nonheme perspective, J. Am. Chem. Soc. 138 (2016) 11410–11428.

[13] R.A. Baglia, J.P.T. Zaragoza, D.P. Goldberg, Biomimetic reactivity of oxygen-derived manganese and iron porphyrinoid complexes, Chem. Rev. 117 (2017) 13320–13352.

[14] E.G. Samsel, K. Srinivasan, J.K. Kochi, Mechanism of the chromium-catalyzed epoxidation of olefins. Role of oxochromium(V) cations, J. Am. Chem. Soc. 107 (1985) 7606–7617.

[15] K. Srinivasan, P. Michand, J.K. Kochi, Epoxidation of olefins with cationic (salen) Mn“' complexes. The modulation of catalytic activity by substituents, J. Am. Chem. Soc. 108 (1986) 2309–2320.

[16] E.N. Jacobsen, Comprehensive Organometallic Chemistry II, in: G.W.S. Wilkinson, F.G.A. Abel, E.W.; Hegedus, L.S. (Eds.), Pergamon, New York, 1995, pp. 1097.

[17] T. Katsuki, Catalytic asymmetric oxidations using optically active (salen)manganese (III) complexes as catalysts, Coord. Chem. Rev. 140 (1995) 189–214.

[18] E.M. McGarrigle, D.G. Gilheany, Chromium− and Manganese−salen Promoted Epoxidation of Alkenes, Chem. Rev. 105 (2005) 1563–1602.

[19] T. Katsuki, Some recent advances in meallosalen chemistry, Synlett (2003) 281–297.

[20] W. Zhang, J.L. Loebach, S.R. Wilson, E.N. Jacobsen, Enantioselective epoxidation of unfunctionalized olefins catalyzed by salen manganese complexes, J. Am. Chem. Soc. 112 (1990) 2801–2803.

[21] R. Irie, K. Noda, Y. Ito, T. Katsuki, Enantioselective epoxidation of unfunctionalized olefins using chiral (salen)manganese(III) complexes, Tetrahedron Lett. 32 (1991) 1055–1058.

[22] Y. Tehshik, E.N. Jacobsen, Privileged chiral catalyst, Science 299 (2007) 1691–1693.

[23] S. Shaw, J.D. White, Asymmetric catalysis using chiral salen-metal complexes: recent advances, Chem. Rev. 119 (2019) 9381–9426.

[24] N.S. Venkataramanan, G. Kuppuraj, R. Rajagopal, Metal–salen complexes as efficient catalysts for the oxygenation of heteroatom containing organic compounds—synthetic and mechanistic aspects, Coord. Chem. Rev. 249 (2005) 1249–1268.

[25] D. Feichtinger, D.A. Plattner, Probing the reactivity of oxomanganeseÿsalen complexes: an electrospray tandem mass spectrometric study of highly reactive intermediates, Chem. A Euro. J. 7 (2001) 591–599.

[26] S.-Y. Liu, J.D. Soper, J.Y. Yang, E.V. Rybak-Akimova, D.G. Nocera, Mechanistic studies of hangman salophen-mediated activation of O-O bonds, Inorg. Chem. 45 (2006) 7572–7574.

[27] Y. Huang, E. Vanover, R. Zhang, A facile photosynthesis of trans-dioxoruthenium (VI) porphyrins, Chem. Commun. 46 (2010) 3776–3778.

[28] R. Zhang, E. Vanover, W.-L. Luo, M. Newcomb, Photochemical generation and kinetic studies of a putative porphyrin-ruthenium(V)-oxo species, Dalton Trans. 43 (2014) 8749–8756.

[29] T.H. Chen, N. Asiri, K.W. Kwong, J. Malone, R. Zhang, Ligand control in the photochemical generation of high-valent porphyrin-iron–oxo derivatives, Chem. Commun. 51 (2015) 9949–9952.

[30] K.W. Kwong, N.F. Lee, D. Ranburg, J. Malone, R. Zhang, Visible light-induced formation of corrole-manganese(V)-oxo complexes: observation of multiple oxidation pathways, J. Inorg. Biochem. 163 (2016) 39–44.

[31] K.W. Kwong, C.M. Winchester, R. Zhang, Photochemical generation of manganese (IV)-oxo porphyrins by visible light photolysis of dimanganese(III) l-oxo bis-porphyrins, Inorg. Chim. Acta 451 (2016) 202–206.

[32] N.F. Lee, J. Malone, H. Jeddi, K.W. Kwong, R. Zhang, Visible-light photolysis of corrole-manganese(IV) nitrites to generate corrole-manganese(V)-oxo complexes, Inorg. Chem. Commun. 82 (2017) 27–30.

[33] R. Zhang, J.H. Horner, M. Newcomb, Laser flash photolysis generation and kinetic studies of porphyrin-manganese-oxo intermediates. rate constants for oxidations effected by porphyrin-MnV-Oxo species and apparent disproportionation equilibrium constants for porphyrin-MnIV-Oxo species, J. Am. Chem. Soc. 127 (2005) 6573–6582.

[34] Z. Pan, R. Zhang, L.W.M. Fung, M. Newcomb, Photochemical production of a highly reactive porphyrin-iron-oxo species, Inorg. Chem. 46 (2007) 1517–1519.

[35] Z. Pan, Q. Wang, X. Sheng, J.H. Horner, M. Newcomb, Highly reactive porphyrin−iron−oxo derivatives produced by photolyses of metastable porphyrin−iron (IV) diperchlorates, J. Am. Chem. Soc. 131 (2009) 2621–2628.

[36] R. Zhang, M. Newcomb, Laser flash photolysis generation of high-valent transition metal-oxo species: insights from kinetic studies in real time, Acc. Chem. Res. 41 (2008) 468–477.

[37] J. Cheng, K. Wei, X. Ma, X. Zhou, H. Xiang, Synthesis and photophysical properties of colorful salen-type schiff bases, J. Phys. Chem. C 117 (2013) 16552–16563.

[38] A.S. Faponle, M.G. Quesne, C.V. Sastri, F. Banse, S.P. de Visser, Differences and comparisons of the properties and reactivities of iron(III)–hydroperoxo complexes with saturated coordination sphere, Chem. Eur. J. 21 (2015) 1221–1236.

[39] K.W. Kwong, D. Patel, J. Malone, N.F. Lee, B. Kash, R. Zhang, An investigation of ligand effects on the visible light-induced formation of porphyrin–iron(IV)-oxo intermediates, New J. Chem. 41 (2017) 14334–14341.

[40] R. Zhang, Y. Huang, C. Abebrese, H. Thompson, E. Vanover, C. Webb, Generation of trans-dioxoruthenium(VI) porphyrins: a photochemical approach, Inorg. Chim. Acta 372 (2011) 152–157.

[41] N.-F. Lee, D. Patel, H.Y. Liu, R. Zhang, Insights from kinetic studies of photo-generated compound II models: reactivity toward aryl sulfides, J. Inorg. Biochem. 183 (2018) 56–65.

[42] R. Sevvel, S. Rajagopal, C. Srinivasan, N. Ismail Alhaji, A. Chellamani, Mechanism of selective oxidation of organic sulfides with oxo(salen)chromium(V) complexes, J. Org. Chem. 65 (2000) 3334–3340.

[43] C. Abebrese, Y. Huang, A. Pan, Z. Yuan, R. Zhang, Kinetic studies of oxygen atom transfer reactions from trans-dioxoruthenium(VI) porphyrins to sulfides, J. Inorg. Biochem. 105 (2011) 1555–1561.

[44] S. Otocka, M. Kwiatkowska, L. Madalinska, P. Kielbasinski, Chiral organosulfur ligands/catalysts with a stereogenic sulfur atom: applications in asymmetric synthesis, Chem. Rev. 117 (2017) 4147–4181.

[45] X. Xue, W. Zhao, B. Ma, Y. Ding, Efficient oxidation of sulfides catalyzed by a temperature-responsive phase transfer catalyst [(C18H37)2(CH3)2N]7 PW11O39 with hydrogen peroxide, Catal. Commun. 29 (2012) 73–76.

[46] W. Zhao, C. Yang, Z. Cheng, Z. Zhang, A reusable catalytic system for sulfide oxidation and epoxidation of allylic alcohols in watercatalyzed by poly(dimethyl diallyl) ammonium/polyoxometalate, Green Chem. 18 (2016) 995–998.

[47] W. Zhao, C. Yang, X. Sun, Z. Cheng, T. Chang, Green catalysis for the selective oxidation of sulfides with high turnover numbers in water at room temperature, New J. Chem. 42 (2018) 19349–19352.

[48] K.W. Kwong, T.H. Chen, W. Luo, H. Jeddi, R. Zhang, A biomimetic oxidation catalyzed by manganese(III) porphyrins and iodobenzene diacetate: Synthetic and mechanistic investigations, Inorg. Chim. Acta 430 (2015) 176–183.

[49] J.H. In, S.E. Park, R. Song, W. Nam, Iodobenzene diacetate as an efficient terminal oxidant in iron(III) porphyrin complex-catalyzed oxygenation reactions, Inorg. Chim. Acta 343 (2003) 373–376.

[50] T.-H. Chen, K.-W. Kwong, A. Carver, W.L. Luo, R. Zhang, Enhanced iron(III) corrole-catalyzed oxidations with iodobenzene diacetate: Synthetic and mechanistic investigations, Appl. Catal. A 497 (2015) 121–126.

[51] T.H. Chen, K.W. Kwong, N.G. Lee, D. Ranburger, R. Zhang, Highly efficient and chemoselective oxidation of sulfides catalyzed by iron(III) corroles with iodobenzene diacetate, Inorg. Chem. Acta 451 (2016) 65–72.

[52] D. Ranburger, B. Willis, B. Kash, H. Jeddi, C. Alcantar, R. Zhang, Synthetic and mechanistic investigations on manganese corrole-catalyzed oxidation of sulfides with iodobenzene diacetate, Inorg. Chem. Acta 487 (2019) 41–49.

[53] D. Ranburger, B. Willis, B. Kash, H. Jeddi, C. Alcantar, R. Zhang, Synthetic and mechanistic investigations on manganese corrole-catalyzed oxidation of sulfides with iodobenzene diacetate, Inorg. Chim. Acta 487 (2019) 41–49.

[54] A. Mahammed, H.B. Gray, A.E. Meier-Callahan, Z. Gross, Aerobic oxidations catalyzed by chromium corroles, J. Am. Chem. Soc. 125 (2003) 1162–1163.

[55] Although asymmetric catalytic sulfoxidation by chiral salen catalysts is beyond the scope of the current study, assessment of the enantioselectivity in catalytic and stoichiometric sulfoxidations by salen-chromium(V)-oxo could provide an alternative way to prove different oxidants involved.

[56] S.H. Wang, B.S. Mandimutsira, R. Todd, B. Ramdhanie, J.P. Fox, D.P. Goldberg, Catalytic sulfoxidation and epoxidation with a Mn(III) triazacorrole: evidence for a “third oxidant” in high-valent porphyrinoid oxidations, J. Am. Chem. Soc. 126 (2004) 18–19.